

CANCOM2024 – CANADIAN INTERNATIONAL CONFERENCE ON COMPOSITE MATERIALS
**FAILURE MODE PREDICTION OF 2D TUBULAR BRAIDED
COMPOSITES WITH TWISTED FIBERS AND GRAPHENE INFUSED
EPOXY**

Frandsen, E.¹, Ead, A.S.¹, Carey, J.P.^{1*}

¹Mechanical Engineering, University of Alberta, Edmonton, Canada

* Corresponding author (jpcarey@ualberta.ca)

Keywords: *Nanocomposite, Braid, Shape Efficiency*

ABSTRACT

This study analytically investigates the compressive failure mode of three configurations of para-aramid/epoxy tubular braided composites (TBCs) with and without nanoparticle reinforcements and low angle yarn twist. The three configurations considered were 35°, 45° and 55° braid angles. Classical laminate theory (CLT) was used in conjunction with the Halpin-Tsai empirical model and Fornes and Paul's effective modulus model to find TBC base elastic properties. A modified shape efficiency model adapted to TBCs was subsequently used to predict the failure mode. The configurations were varied by separately testing samples with 5° yarn twist in the para-aramid and the addition of graphene nanoplatelets (GnP) to the epoxy. The results of the model suggest that all presented configurations will fail due to diamond shaped buckling. The results also suggest that twist has a greater effect on the failure mode than the strengthening and stiffening effect of the GnPs. This is attributed to the geometric effect of the fiber twist. While the model seems insensitive to small variations in input values and relatively conclusive in the resultant failure mode, experimental results will be necessary to further validate the conclusions.

1 INTRODUCTION AND BACKGROUND

1.1 Tubular Braided Composites (TBCs)

Composite materials are a tailorable combination of multiple physically bonded materials. TBCs are made by braiding textile fibers into a preform on a cylindrical mandrel and impregnated with a resin. Several parameters of the braiding process can be altered to produce braided preforms of various geometries. Figure 1a shows a model of a biaxial diamond braid with a cross sectional view of the TBC. The braid angle is measured from the deviation of the yarns from the longitudinal axis. Following the manufacture of the preform, it is impregnated with a matrix and cured to make the final TBC. All configurations in this text will be biaxial TBCs with para-aramid yarns (Twaron®) and an Epon™ 826 resin.

1.2 Yarn Twist

Yarn twist is the rotation of a yarn to form a helical angle around the yarn longitudinal axis (see Figure 1b). The influence of yarn twist on the mechanical properties of TBCs has been sparsely investigated. Cheung and Carey looked at the influence of yarn twist on the properties of continuous Kevlar® 49 fibers and to TBCs [1], [2]. Results showed a reduction of yarn fraying during TBC manufacture and that twist decreases the elastic modulus and increases the strength of dry yarns for angles of twist up to 6°. Conversely, twist increases both the elastic

CANCOM2024 – CANADIAN INTERNATIONAL CONFERENCE ON COMPOSITE MATERIALS

modulus and strength of TBCs in tension while changing the geometry of the yarn into an ellipse with tighter foci. This results in TBCs with more inter-yarn spacing creating a more open mesh. Figure 1b shows an example of this change in geometry. However, little is known of its effect in compressive properties.

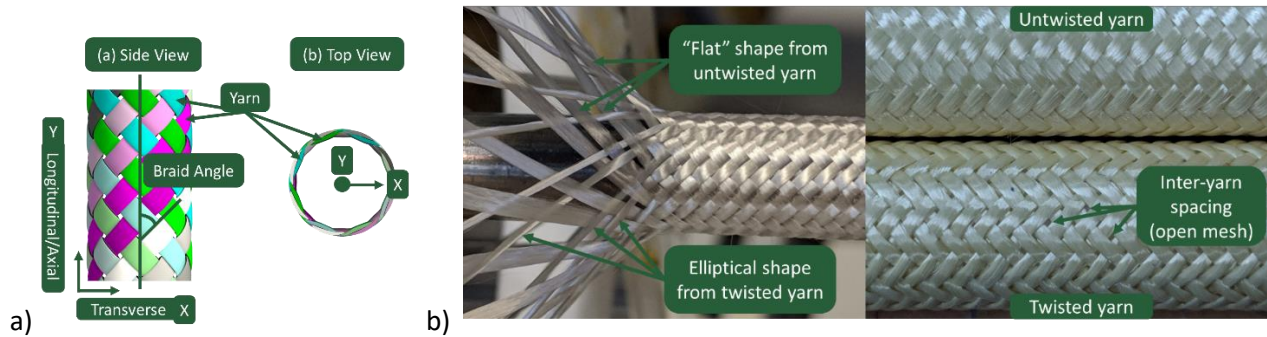


Figure 1. (a) Model of a TBC showing some commonly used terminology. (b) Photo showing the geometric differences between twisted and untwisted yarns in cellulose TBCs [2] (provided by B. Cheung).

1.3 Graphene Nanoplatelet (GnP)

Due to its high specific stiffness [3] GnP, a 2D nanoplatelet form of graphene, has been investigated as a suitable filler reinforcement in composites forming nanocomposites. The research following the initial characterization of GnPs has led to many studies manufacturing GnP-reinforced nanocomposites due to its potential as an electrically and thermally conductive agent in polymers as well as a stiffening reinforcement [4].

1.4 Objectives

This paper focuses on predicting the compressive failure mode of TBCs combined with GnP reinforcements and yarn twist using the shape efficiency model, the Halpin-Tsai empirical model, classical laminate plate theory (CLPT), and Tresca Criterion.

2 THEORETICAL DERIVATION AND MODELLING

2.1 Shape Efficiency Model for a Shape Efficiency Map

Originally proposed by Weaver and Ashby [5] and later adapted to TBCs by Harte and Fleck [6], the shape efficiency model (SEM) describes a shape factor for characterizing the design of an efficient shape for a variety of structural members, depending on stiffness or failure-based criteria [5]. This model enables designing TBCs with required mechanical properties and failure mode by adjusting its overall shape for a given application while keeping the materials to a minimum, which applies well to the low specific strength of advanced composites such as TBCs. For compressive loading scenarios, the compression of thin-walled tubes is failure-based criteria, the SEM uses the different stress-based failure modes - local buckling, global buckling and Euler buckling – and categorizes the structural traits that leads to each mode.

The transition regions between failure modes can be found by equating the failure initiation stresses for each type of compression to each other to find the mathematical boundaries between the modes. With these equalities, the variables can be solved into dimensionless groups based on the load and shape efficiency.

The resulting equations describe a piecewise function predicting the TBC structure's compressive failure compartment within each region. For Euler buckling, diamond buckling and micro buckling, this is respectively [6]:

CANCOM2024 – CANADIAN INTERNATIONAL CONFERENCE ON COMPOSITE MATERIALS

$$\frac{PE^2}{l^2\tau^3} = \frac{\pi}{4} * \left(\frac{mE^2}{\rho l^3 \tau^2} \right) * \frac{\tau\Phi}{E} \quad (1)$$

$$\frac{PE^2}{l^2\tau^3} = 0.6\alpha * \left(\frac{mE^2}{\rho l^3 \tau^2} \right) * \frac{E}{\tau\Phi} \quad (2)$$

$$\frac{PE^2}{l^2\tau^3} = \left(\frac{mE^2}{\rho l^3 \tau^2} \right) * \frac{1}{\tan(\varphi)} \quad (3)$$

where E is the compressive elastic modulus, P is the load at which collapse occurs, m is the TBC mass, ρ is the density, Φ is the dimensionless shape efficiency described by Weaver and Ashby [5], l is the length of the TBC, α is the dimensionless knockdown factor which accounts for the structure anisotropy. Young suggested a value of 0.5 for α which was later adjusted to 0.5-0.8 by Weingarten et al. due to the influence of imperfections in the TBC wall [7]. τ is the matrix shear strength and φ is the fiber “waviness”.

The shape efficiency, Φ , is heavily dependent on the waviness and knockdown factor as determinants of the boundaries of the failure regions. Harte and Fleck found through experiments that the waviness, which is the fiber deviation from its normal path, was consistently around 10° [6] which will be assumed herein. Regarding the knockdown factor, this analysis will assume the value put forth by Young of 0.5 and compare it to the high α described by Weingarten et al., 0.8.

It is important to note that equations (1)-(3) have been organized into dimensionless factors. These are known as the mass factor, MF , load factor, LF , and shape factor, SF , and subsequently allows the plotting of structures on a shape efficiency map put forth by Weaver and Ashby [5]. Assuming the sample fails under either micro buckling or diamond buckling (since l was chosen to be relatively small), the SF can be compared to the boundary between micro buckling and diamond buckling to determine the final compressive equation to use. With this, the points can be plotted on a shape efficiency map.

2.2 Composite Moduli Models

To calculate the elastic moduli for the shape efficiency model, the empirical model by Halpin and Tsai [8] is used for nanocomposites with the proper reinforcing factor [4], [9]. It has not been applied extensively to the shear modulus in nanocomposites. Since the Halpin-Tsai model uses the same equations for both shear and elastic moduli [4], [9], the same reinforcing factor was applied to the shear modulus. Validation was conducted to confirm the sensitivity of the modeled properties to changes in the shear modulus.

The crucial unknown in the Halpin-Tsai equations is the reinforcing factor dependent on the filler geometry and orientation. GnPs are assumed to be a thin disc with a high aspect ratio. To derive values for the reinforcing factor, the platelet is defined in the radial and axial directions [9]. When platelets are loaded in the radial directions the reinforcing factor is 2 and axial is 2/3 the aspect ratio of the platelet [4].

Although the Halpin-Tsai equations, may be used to calculate the modulus of a nanoparticle reinforced composite with either uniformly transverse or longitudinal platelets, the effective mean model is a method for estimating the modulus of a 3D randomly distributed nanocomposite [9], [10]. In this model, a multi-step random orientation of

CANCOM2024 – CANADIAN INTERNATIONAL CONFERENCE ON COMPOSITE MATERIALS

the nanoplatelets developed by Van Es [10] approximates both the transverse and longitudinal moduli in conjunction to get an empirical equation for the modulus based off the nanocomposite geometry.

The final model used in this analysis was developed by Carey et al. [11] based on CLPT for the estimation of TBC mechanical properties based of the matrix and fiber constituents. This model uses a flat unit cell to find the aggregate properties of each region and its respective geometry. The TBC properties are then integrated into the SEM.

2.3 Shear Strength

Shear strength of the composite is essential to apply the shape efficiency model to nano reinforced TBCs; however, it is difficult to predict or analyze. Most models vary drastically in their accuracy and typically apply to specific materials or load states [6], [12] This work uses the Tresca yield criterion which typically applies to ductile materials [12]. Epon 826 exhibits ductile yield before experiencing brittle fracture, and it has been shown to agree with Tresca criterion during yield. It estimates the maximum in-plane shear stress as half the ultimate tensile strength. This paper will use an improved shear strength of 2.5 MPa.

3 METHODOLOGY

3.1 Materials

Twaron®/Epon™ 826 (TE), 5° twisted Twaron®/Epon™ 826 (TTE) and Twaron®/Epon™ 826/Graphene (TEG) composites were used in this study at three braid angles (35°, 45° and 55°) for a total of 9 configurations. The base properties of the materials used can be seen in Table 1.

Table 1. Material base properties.

	Materials			
	Twaron® [13]	5° Twisted Twaron® [1], [13]	Epon™ 826/LS 81K Hardener [14]	GnP [15]
Elastic Modulus [GPa]	99	98	2.73	250
Density [g/cm³]	1.44	1.44	1.16	2.2

3.2 Modeling

The models were programmed using MATLAB® 2022b [16]. Nanocomposite mixture of GnP with Epoxy was analyzed using the Halpin-Tsai empirical model with the effective mean modulus to determine the matrix properties [8], [9]. The properties for all configurations were input into the CLPT model for composite elastic properties [11]. Finally, all the necessary variables were input into the modified shape efficiency model by Harte and Fleck to calculate the final shape efficiency map and failure mode regions [6].

4 RESULTS AND DISCUSSION

Using the methodology highlighted in section 3, shape efficiency maps were plotted. Figure 2a shows the shape efficiency map and compares it to variations in the waviness and knockdown factor. If the waviness is halved, there is a lower misalignment in the yarn fibers and the sample will be less likely to fail due to micro buckling. Conversely, the micro buckling region grows with a larger waviness. The knockdown causes samples to be more likely to fail in micro buckling since it means there are likely more/larger imperfections in the tube wall. The overall shape of the map, however, remains constant with a change in the waviness and knockdown factor.

CANCOM2024 – CANADIAN INTERNATIONAL CONFERENCE ON COMPOSITE MATERIALS

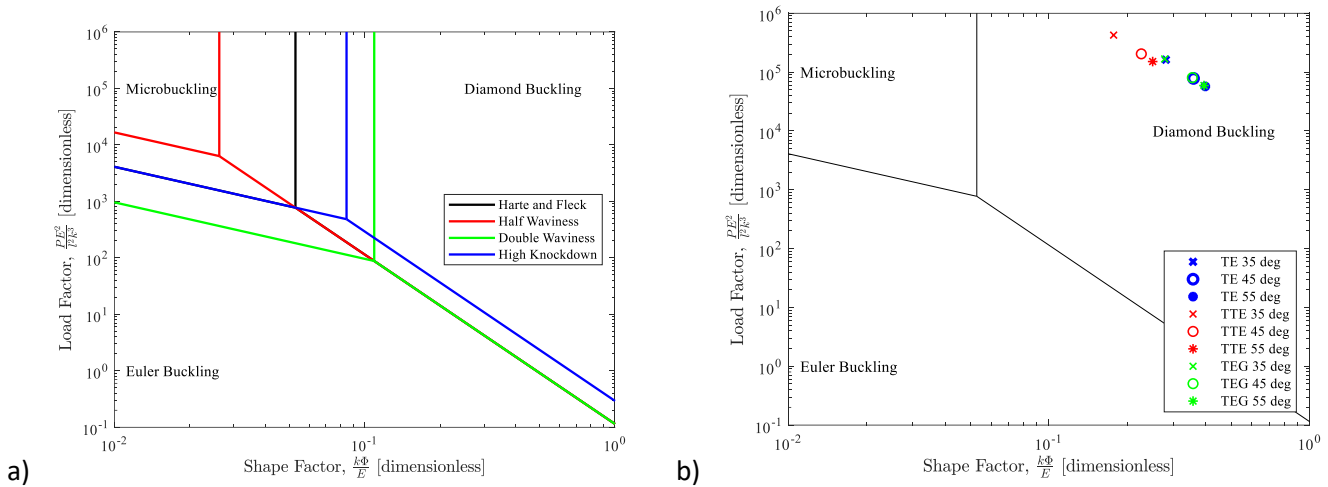


Figure 2. Modified shape efficiency a) comparison of key variables, waviness and alpha adjusted to study their effect of the region shapes, b) for the presented configurations. Note that the TE points are very close in value to the TEG values.

Figure 2b shows the shape efficiency map with the points for the chosen configurations. The MF contours are not included in the plot, however the contour lines in the diamond buckling region are nearly parallel to the shape of the boundary between diamond and Euler buckling. This implies that the chosen samples all fall around the same MF as expected. We note that the slight change in geometry from the twisted samples (TTE) seems to have a much greater effect on the failure than the increased stiffness from the twisted/graphene (TEG) composite. Consequently, the results of this work suggest that the addition of GnP in the matrix causes samples to approach the micro buckling mode despite the higher shear strength and higher stiffness.

The presented analysis predicts the compressive failure of TBC samples using mechanical properties obtained through multiple predictive models. While the predictions in this analysis are justifiable, there are a few aspects that are difficult to predict analytically. Shear strength is a significant limiting factor in this analysis. The interactions of the material in tension may not lead to a direct increase of shear strength as was assumed here. Shear modulus properties of TBCs have not been investigated as thoroughly as the tensile elastic modulus.

Knockdown factor is another assumption that affects the result of its model as shown in figure 2a. Waviness is approximated from literature but largely dependent on many variables. However, the chosen braid samples seem insensitive to minor variations in the independent variables. With a very high tube radius to wall thickness ratio, defined as the shape efficiency herein, the tube is considered thin walled. This ratio would have to change significantly to approach the failure boundary and alter its mode. As shown, adjusting the wall thickness or radius alone will change the shape efficiency and the failure mode. Conversely, the addition of GnP has limited effects on TBC properties since the properties are already dominated by the impregnated textile material, and thus does not change failure modes. Significant changes in the failure mode would require adjusting the primary materials (yarn or matrix) or shifting the geometric properties.

5 CONCLUSION

This paper presents an analysis of the shape efficiency model adapted to TBCs and attempts to predict the failure mode of different configurations of para-aramid/epoxy TBCs reinforced with GnPs [6]. The configurations include

CANCOM2024 – CANADIAN INTERNATIONAL CONFERENCE ON COMPOSITE MATERIALS

a traditional TBC, a TBC with twisted yarns and a traditional TBC with a GnP reinforced nanocomposite matrix. The resultant shape efficiency map suggests that the presented sample configurations will all fail in diamond shaped buckling. Despite the lack of sensitivity of the model to small variations in mechanical properties, several assumptions made in this work need to be further investigated. Additionally, experimental validation of the results presented should be conducted.

6 ACKNOWLEDGMENT

The authors acknowledge the support of Kate Bennett and Mrittika Mamun. Funded by NSERC Discovery Grant RGPIN-2022-03043.

7 REFERENCES

- [1] B. K. O. Cheung and J. P. Carey, "Characterizing and modeling of low twist yarn mechanics," *J Eng Fiber Fabr*, vol. 14, Jul. 2019, doi: 10.1177/1558925019866945.
- [2] B. K. O. Cheung and J. P. Carey, "Improving two-dimensional braided composite tensile properties by including low angle yarn twist: Production, experimental verification, and modeling," *J Eng Fiber Fabr*, vol. 15, 2020, doi: 10.1177/1558925020946449.
- [3] C. N. R. Rao, A. K. Sood, K. S. Subrahmanyam, and A. Govindaraj, "Graphene: The new two-dimensional nanomaterial," *Angewandte Chemie - International Edition*, vol. 48, no. 42, pp. 7752–7777, Oct. 2009, doi: 10.1002/anie.200901678.
- [4] P. G. Ren, D. X. Yan, T. Chen, B. Q. Zeng, and Z. M. Li, "Improved properties of highly oriented graphene/polymer nanocomposites," *J Appl Polym Sci*, vol. 121, no. 6, pp. 3167–3174, Sep. 2011, doi: 10.1002/app.33856.
- [5] P. M. Weaver and M. F. Ashby, "MATERIAL LIMITS FOR SHAPE EFFICIENCY," 1998.
- [6] A. M. Harte and N. A. Fleck, "DEFORMATION AND FAILURE MECHANISMS OF BRAIDED COMPOSITE TUBES IN COMPRESSION AND TORSION," 2000. [Online]. Available: www.elsevier.com/locate/actamat
- [7] V. I. Weingarten, P. Seide, and J. P. Peterson, "Buckling of Thin-Walled Circular Cylinders," 1968.
- [8] A. K. Kaw, *Mechanics of composite materials*. Taylor & Francis, 2006.
- [9] T. D. Fornes and D. R. Paul, "Modeling properties of nylon 6/clay nanocomposites using composite theories," *Polymer (Guildf)*, vol. 44, no. 17, pp. 4993–5013, Aug. 2003, doi: 10.1016/S0032-3861(03)00471-3.
- [10] M. A. van Es, *Polymer-clay nanocomposites : the importance of particle dimensions*. s.n., 2001.
- [11] J. P. Carey, *Handbook of Advances in Braided Composite Materials : Theory, Production, Testing and Applications*. Elsevier Science, 2016.
- [12] Y. Hu, Z. Xia, and F. Ellyin, "The Failure Behavior of an Epoxy Resin Subject to Multiaxial Loadings," 2006.
- [13] "Product data sheet PARA-ARAMID FIBER."
- [14] "Starting Formulation SF 8017 Epoxy Resin System for Pultrusion or Filament Winding EPON™ Resin 826 or EPON™ Resin 862 / LS-81K Anhydride Curing Agent (MTHPA)."
- [15] A. J. Bourque, C. R. Locker, A. H. Tsou, and M. Vadlamudi, "Nucleation and mechanical enhancements in polyethylene-graphene nanoplate composites," *Polymer (Guildf)*, vol. 99, pp. 263–272, Sep. 2016, doi: 10.1016/j.polymer.2016.07.025.
- [16] "MATLAB®." MathWorks, Natick, Massachusetts, 2022.